ELSEVIER

Catalysis Today 68 (2001) 41–51

CATALYSIS TODAY

www.elsevier.com/locate/cattod

Platinum catalysts supported on Al-pillared clays Application to the catalytic combustion of acetone and methyl-ethyl-ketone

A. Gil [a,*], M.A. Vicente [b], J.-F. Lambert [c], L.M. Gandía [a,1]

[a] *Departamento de Química Aplicada, Edificio Los Acebos, Universidad Pública de Navarra, Campus de Arrosadía s/n, E-31006 Pamplona, Spain*

[b] *Departamento de Química Inorgánica, Facultad de Ciencias Químicas, Universidad de Salamanca, Plaza de la Merced s/n, E-37008 Salamanca, Spain*

[c] *Laboratoire de Reactivité de Surface, Université Pierre et Marie Curie, 4 Place Jussieu, Tour 54, Casier 178, 75252 Paris Cedex 05, France*

Abstract

A hectorite, a montmorillonite and a saponite, all of them in their Al-pillared forms, as well as unpillared saponite were considered as supports of platinum catalysts (2.3 wt.% Pt) for the catalytic combustion of acetone and methyl-ethyl-ketone (MEK). The preparation of the catalysts modified the textural properties of the Al-pillared clay supports, giving rise to a significant loss of specific surface area and micropore volume. After hydrogen reduction at 773 K, the presence of poorly dispersed metallic platinum with mean crystallite sizes in the 70–100 Å range was detected by X-ray diffraction (XRD). Good activity and stability performances were found under the reaction conditions used. Whatever be the catalyst considered, MEK resulted easier to oxidize than acetone, a fact which has been related to the strength of the weakest C–H bond in these ketones. Remarkable differences in catalytic activity arose depending on the pillared or unpillared character of the support and the nature of the starting smectite clay used. Regardless of the ketone molecule, the following order of decreasing catalytic performance was established with respect to the support nature: unpillared saponite > Al-pillared montmorillonite > Al-pillared saponite > Al-pillared hectorite.

Keywords: Al-pillared clays; Acetone catalytic combustion; Methyl-ethyl-ketone catalytic combustion; Platinum catalysts

1. Introduction

Pillared interlayered clays (PILCs), or pillared clays, constitute an important family of high surface area microporous materials. They are prepared by exchanging the charge-compensating cations present in the interlamellar space of the parent clays with bulky inorganic polyoxocations formed by hydrolysis of some metal salts. Upon calcination these polyoxocations undergo limited structural transformations and are converted to metal oxyhydroxide clusters, named pillars, that keep the clay layers apart thus preventing their collapse and cannot be back-exchanged any more due to the formation of covalent bonds with the layers. The result is a stable material with acidic properties and a two-dimensional porous structure of molecular dimensions defined by the interlayer and interpillar spacings [1–8]. Layered silicates of the smectite class

* Corresponding author. Tel.: +34-948-169-605; fax: +34-948-169-606.
E-mail addresses: andoni@unavarra.es (A. Gil), lgandia@unavarra.es (L.M. Gandía).
[1] Co-corresponding author. Tel.: +34-948-169-605; fax: +34-948-169-606.

0920-5861/01/$ – see front matter
PII: S0920-5861(01)00321-2

are naturally occurring clays which have been widely utilized in the preparation of PILCs. These materials belong to the category of the 2:1-phyllosilicates whose basal layer is constituted by a sheet of $M(O, OH)_6$ octahedra (where $M = Al^{3+}, Mg^{2+}, Fe^{3+}$ or Fe^{2+}) sandwiched between two sheets of $Si(O, OH)_4$ tetrahedra. Montmorillonite, saponite, and less frequently hectorite and beidellite are the main smectites employed in pillaring studies [7,9,10].

Although the pillaring of smectites with polyoxocations formed upon the hydrolysis of salts of several elements, such as Al^{3+}, Cr^{3+}, Fe^{3+}, Ga^{3+}, Si^{4+}, Ti^{4+} and Zr^{4+}, has been described, only in the case of Al- and Ga-based polyoxocations there is unequivocal knowledge of the main pillaring species involved [2,5,8]. Thus, it is well known that in the typical pillaring solutions (with an OH^-/Al^{3+} ratio of about 2.2) often used to prepare Al-PILCs, most of the Al^{3+} is in the form of the tridecamer $[Al_{13}O_4(OH)_{24}(H_2O)_{12}]^{7+}$, usually denoted as Al_{13}, which is the main pillaring species in this case. It should be noted that, nowadays, smectites pillared with Al_{13} are the only PILCs for which reliable relationships between acidity and structural characteristics can be established [5], and for which the effect of the preparation conditions on the resulting textural properties is well understood [11–14].

Due to their acid properties and open microporosity, Al- and Zr-PILCs were first considered as promising cracking catalysts for relatively large organic molecules; however, they presented several major drawbacks that seriously limited this application [2]. Nevertheless, these solids still demonstrated considerable potential to take part in the preparation of catalysts for some types of acid-catalysed reactions [5,7,8,10]. The scope of the potential catalytic applications of PILCs has expanded considerably in recent years as the fact that pillars prop the clay layers apart has been recognized as only one point of view. In fact, it may also be said that the clay layers keep the pillars apart, and accordingly the microstructure is interpreted in terms of the presence in the interlayer space of an ultradisperse oxide phase [5]. Hence, the pillaring of clays with polyoxocations of several transition metals (Cr, Fe, Ti) or with mixed Al–M systems (M = Cr, Cu, Fe, Mo, Ru) has allowed new catalytic functions to be incorporated into PILCs. The potentialities of these solids as catalysts for hydrogenation–dehydrogenation, Fischer–Tropsch, isomerization, hydrodesulphurization, NO selective catalytic reduction, selective and complete hydrocarbon oxidation processes, among others, have been explored [8]. Regarding Al-PILCs, the pillars can be also considered as a hydroxy-aluminic phase with particles of nano- or subnanometric scale that is incorporated in the interlayer space of the clays [15]. Interestingly, Al-PILCs sometimes exhibit physico-chemical properties such as acid characteristics, reminiscent of a conventional alumina-support surface [5]. This view may also be applied to Zr-PILCs; e.g., it has been found that manganese oxide catalysts supported on Al- and Zr-pillared montmorillonite and saponite behave similarly to manganese oxides dispersed on conventional alumina and zirconia supports [16]. In recent years, the number of studies dealing with the use of PILCs as supports to achieve homogeneous dispersion of catalytically active phases has rapidly grown. The main aspects of the preparation, characterization and applications of these catalysts have been recently reviewed [8].

In this paper, we present and discuss the preliminary results of a study on the use of several Al-pillared smectites (a hectorite, a montmorillonite and a saponite) as supports of platinum catalysts for the catalytic combustion of volatile organic compounds (VOCs); in this case, of two carbonyl VOCs, acetone and MEK. Catalytic combustion is a well-established technology for controlling VOC and odour emissions which has been successfully applied in a wide range of commercial installations [17,18]. Noble metals, typically Pt or Pd in monometallic form, bimetallic Pt–Pd mixtures or noble metals in combination with some metal oxides, are usually the preferred active phases as VOC combustion catalysts [17,19–21]. This is mainly due to their high specific activity that generally allows lower operating temperatures and higher space velocities for a given VOC destruction efficiency compared to the transition metal oxide-based catalysts. In contrast to the case of alkanes and aromatic hydrocarbons, the catalytic combustion of carbonyl compounds has not been extensively studied. However, some of these compounds, such as MEK, are common solvents used in many industrial processes that contribute significantly to VOC emissions [17].

The reason for considering several smectites in this work was to explore the effect of the nature

of the parent clay in the catalytic performance of the supported catalysts. In this respect, it should be noted that, based on the number of octahedral sites per unit cell occupied, montmorillonite is a dioctahedral smectite (two-thirds of the octahedral holes are occupied in the idealized structure), whereas both hectorite and saponite show trioctahedral occupancy (all the octahedral holes are occupied in the idealized structure) [7]. Moreover, regarding isomorphous substitution, it takes place majoritarily in the tetrahedral sheets of saponite; but in contrast, in hectorite and montmorillonite the octahedral sheets are involved. Therefore, the negative charge of the layer is mainly localized on the tetrahedral sheets of saponite but in the octahedral sheets in the case of montmorillonite and hectorite. To our knowledge, this is the first study dealing with VOC combustion over platinum catalysts supported on PILCs. In two previous works, PILCs were used directly as VOC combustion catalysts. This was the case of methylene chloride combustion over Al-, Al–Fe-, Al–Ru- and Al–Cr-pillared bentonite [22], and acetone combustion over Al-, Cr- and Al–Cr-pillared saponites [23].

2. Experimental

2.1. Al-PILCs synthesis and catalysts preparation

The first stage of the catalyst preparation process was the synthesis of the Al-pillared clays that were subsequently used as catalytic supports. Three natural smectite clays were selected as starting materials, namely, a hectorite from San Bernadino (California, USA), a montmorillonite from Cheto (Arizona, USA) and a saponite from Ballarat (California, USA). The clays were supplied by the Clay Minerals Repository (University of Missouri–Columbia, USA). The as-received materials were purified by careful aqueous dispersion and decantation and the fractions with particle size lesser than 2 μm separated and subjected to intercalation with aluminium oligomers. In order to perform this, an aluminium polycation solution was prepared by slow titration of a solution of $AlCl_3{\cdot}6H_2O$ (Prolabo, 99%) with a 1 M NaOH (Prolabo *Titrinorm*) solution under vigorous stirring, using a OH^-/Al^{3+} mole ratio of 2.2 (pH 4.1). The hydrolysed solution was allowed to age for 24 h at room temperature under constant agitation. The resulting hydroxy-aluminium solution was added to previously prepared suspensions (1% in weight) of the purified clays in deionized water at an Al^{3+}/clay ratio of 5 mmol Al g_{clay}^{-1}. The slurries were stirred for 24 h at room temperature and then centrifuged and washed by dialysis with distilled water until no chloride was present in the filter wash water. The resulting intercalated clays were dried in air at 323 K for 16 h and then calcined under a dry air flow for 4 h at 673 K (hectorite) or 773 K (montmorillonite and saponite) in order to obtain the Al-PILCs. These solids are designated as SBhec-Al, CHmont-Al and BAsap-Al with reference to the Al-pillared San Bernadino hectorite, Al-pillared Cheto montmorillonite and Al-pillared Ballarat saponite, respectively.

Supported platinum catalysts were prepared by wet impregnation of the Al-PILCs with an aqueous solution of $[Pt(NH_3)_4]Cl_2$ (Alfa). The slurries were evaporated slowly under reduced pressure in a rotavapor and the solids thus obtained were finally calcined in air at 773 K for 4 h to yield the Pt/SBhec-Al, Pt/CHmont-Al and Pt/BAsap-Al catalysts. A platinum catalyst (Pt/BAsap) was also prepared as described above by wet impregnation of the unpillared Ballarat saponite. The final amount of Pt in the impregnated solids is equivalent to 2.3 wt.%, and it was chosen considering the amount of Al fixed by the intercalated solids by the following way. First, the amount of Al fixed during the intercalation was analysed: 4.6 wt.% for SBhec-Al, 5.3 wt.% for CHmont-Al and 4.8 wt.% for BAsap-Al, all of them normalised taken the amount of Si in each clay as reference. The lower amount was chosen and the number of Al-pillars corresponding to this amount was calculated, assuming for them the formula of the Al_{13} units. Then, the solids were impregnated with the same number of moles of $[Pt(NH_3)_4]Cl_2$. Thus, for Pt/SBhec-Al, a ratio $Pt/Al_{13} = 1.0$ was used. In the other catalysts, as the number of Al_{13} units is slightly higher, the Pt/Al_{13} ratio is slightly lower, but the maintenance of the final Pt content was preferred.

2.2. Characterization techniques and catalytic activity measurements

Nitrogen adsorption experiments were performed at 77 K using a static volumetric apparatus (Micromeritics ASAP 2010 adsorption analyser). The samples (200 mg) were previously degassed (less than 0.1 Pa)

at 473 K for 24 h. Nitrogen adsorption data were collected in the relative pressure (p/p^0) range 10^{-5}–0.99 by adding successive doses of nitrogen of 4 cm^3 STP g^{-1} until $p/p^0 = 0.01$ was reached. Subsequently, further nitrogen was added and the volumes required to achieve a pre-established set of (p/p^0) values were measured. Specific total surface areas (A_{Lang}) were calculated based on the adsorption data in the (p/p^0) interval of 0.01–0.05 and using the Langmuir equation. Specific total pore volumes (V_p) were estimated from nitrogen uptake at (p/p^0) of about 0.99. On the other hand, the specific micropore volumes ($V_{\mu p}$) were estimated according to the approach of Gil and Grange [24] to the Horvath–Kawazoe method [25] for calculating the micropore size distributions.

X-ray diffraction (XRD) patterns were obtained by using a Siemens D-5000 diffractometer employing nickel-filtered Cu Kα radiation and operating at 20 kV and 30 mA. The equipment was connected to a DACO-MP microprocessor and used Diffract-AT software. The mean metallic platinum (Pt^0) crystallite diameters (d_{Pt}) were estimated from the application of the Scherrer equation [26] to the XRD patterns of the platinum catalysts previously reduced in hydrogen at 773 K. XRD line broadening (XRDLB) measurements were carried out using the Pt^0 (1 1 1) peak (39.8° in 2θ). The width at half-maximum of this peak was corrected for instrumental broadening.

Acetone and MEK combustion reactions were carried out in a tubular (8 mm i.d.) fixed-bed Pyrex glass reactor at atmospheric pressure. The catalyst (50 mg, 100–200 μm particle size fraction) was diluted with inert solids (100–200 μm Pyrex glass beads) in a volume ratio of 1:5 approximately. A thermocouple placed inside the reactor, in the centre of the catalyst bed, monitored the reaction temperature. Mass flow controllers (Bronkhorst) monitored and controlled the flow of gases used to obtain the feed mixture and to pretreat the catalyst. An air stream saturated with the corresponding ketone (Panreac, PA) was created using a saturator equipped with temperature and pressure control, and then diluted with pure air (SEO 99.999%), resulting in a 600 ppmv ketone concentration in the reactor feed. Prior to each experiment, the catalyst was treated under 100 cm^3 min^{-1} of hydrogen (SEO 99.999%) for 1 h at 773 K. The flow was then switched to helium (SEO 99.999%) and the temperature was maintained at 773 K for 15 min. Subsequently, the catalyst was cooled under helium to the desired starting reaction temperature. Prior to obtaining the light-off curves for ketone combustion, the catalytic bed was stabilised for 3 h at 363 K under the feed stream. No oxidation of the ketones was observed during this period. The temperature was then raised at a controlled heating rate of 2.5 K min^{-1} until complete combustion was obtained. A series of long catalytic runs was performed with acetone and the reactor operating at constant combustion temperature of 573 K in order to investigate the catalysts stability. The light-off and stability tests were performed at identical W_{Pt}/F_{in} ratios of 0.153 (g_{Pt} min $mmol^{-1}_{ketone}$) and gas hourly space velocity (GHSV) of about 34 000 h^{-1} (STP) based on the total catalytic bed volume. Some individual experiments that were carried out at the same W_{Pt}/F_{in} ratio but at varying gas linear velocities confirmed the absence of external mass transfer effects. On-line analysis of the product stream was performed on a Hewlett Packard 6890 gas chromatograph, equipped with a 6 ft HayeSep Q column connected to a TCD for CO_2 determination, and an HP-INNOWax 30 m × 0.32 mm i.d. column connected to an FID for ketone analyses.

3. Results and discussion

3.1. Textural properties and mean platinum crystallite diameters

The nitrogen adsorption isotherms at 77 K of the Al-PILCs supports and the corresponding supported platinum catalysts are shown in Fig. 1. At low relative pressures, these isotherms correspond to Type I in the Brunauer, Deming, Deming and Teller classification [27]. Some of the textural properties of the samples derived from the nitrogen adsorption data are given in Table 1, where the specific total surface areas calculated using the Langmuir equation (A_{Lang}), specific total pore volumes (V_p) and micropore volumes ($V_{\mu p}$) are summarized. The values of the basal spacings (d(0 0 1)) of the Al-PILCs determined from the (0 0 1) reflection in the XRD patterns have also been included in Table 1. As can be seen, the samples exhibit basal spacings between 16.9 and 18.4 Å, which correspond to interlayer distances of about 7–9 Å. The Al-PILCs present total specific surface areas close to 200 m^2 g^{-1}

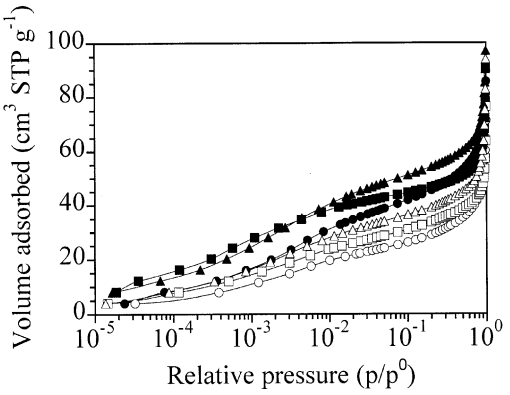

Fig. 1. Nitrogen adsorption isotherms at 77 K: SBhec-Al (●), CHmont-Al (■), BAsap-Al (▲), Pt/SBhec-Al (○), Pt/CHmont-Al (□), and Pt/BAsap-Al (△).

and relatively high specific micropore volumes ranging from 0.072 to 0.084 cm^3 g^{-1}. All these characteristics are similar to those generally found for Al-pillared clays [1–4] and indicate that the catalytic supports used in this work are properly pillared materials.

On comparing the results obtained with the Al-PILCs and the platinum catalysts, it can be observed in Fig. 1 that, whereas the general aspect of the respective adsorption isotherms does not change significantly, a noticeable decrease of the adsorbed nitrogen volume takes place for the supported catalysts in the whole relative pressure range. This fact shows that the presence of dispersed platinum particles has modified the textural properties of the Al-PILC supports, as is also evidenced by the specific surface area and pore volume losses that can be seen in Table 1 for the platinum catalysts. Moreover there is little, if any, influence of the nature of the starting smectite clay on the subsequent evolution of the textural properties during catalyst preparation. A more detailed analysis of the results may be made by comparing for a given Al-PILC the changes in specific total and micropore volume between the support and the respective platinum catalyst. It should also be noted that the specific mesopore volume can be estimated by subtracting the micropore volume from the total pore volume. Hence, it is revealed that the mesopore volume remained almost unchanged and that the pore volume loss suffered by the catalysts almost exclusively affected the micropores of the Al-PILCs. This suggests that in spite of the relatively large mean platinum crystallite diameters found by XRDLB measurements (see Table 1), some platinum species may occupy the inner porous network of the supports after the catalyst preparation process. A very similar evolution of the textural properties with catalyst preparation has been previously reported by Doblin et al. [28] for a Pt/Al-pillared montmorillonite catalyst. Interestingly, in contrast to our case, Doblin et al. loaded the support with a very low Pt content (0.16 wt.%) and reported that the platinum particles were very well dispersed on the catalyst surface.

The mean platinum crystallite diameters exhibited by the catalysts reduced in hydrogen at 773 K range between 71 Å for Pt/BAsap-Al and 98 Å for Pt/BAsap, as indicated in Table 1. These data reveal that platinum is poorly dispersed on the clays surface. As regards the Al-PILCs, it can be said that the nature of the starting smectite has a minor influence on the metallic crystallite diameter resulting after catalyst activation by hydrogen. It seems, on the other hand, that Al-pillaring gives rise to some positive effect as regards platinum

Table 1
Textural properties and mean platinum crystallite diameters of the samples indicated

Sample	$d(0\,0\,1)$ (Å)[a]	A_{Lang} (m^2 g^{-1})[b]	V_p (cm^3 g^{-1})	$V_{\mu p}$ (cm^3 g^{-1})	d_{Pt} (Å)
SBhec-Al	18.4	181 ($C = 255$)[c]	0.132	0.084	–
Pt/SBhec-Al	–	112 ($C = 277$)	0.110	0.061	77
CHmont-Al	16.9	193 ($C = 523$)	0.140	0.072	–
Pt/CHmont-Al	–	132 ($C = 305$)	0.118	0.052	85
BAsap-Al	17.6	222 ($C = 336$)	0.150	0.073	–
Pt/BAsap-Al	–	157 ($C = 300$)	0.145	0.051	71
Pt/BAsap	–	–	–	–	98

[a] Basal spacings of the pillared clays.
[b] $0.01 \leq p/p^0 \leq 0.05$, interval of relative pressure.
[c] Langmuir C-value, characteristic of the intensity of the adsorbate–adsorbent interactions.

distribution, since on using an unpillared clay as support (Pt/BAsap) the mean platinum crystallite diameter increased significantly. As a first approach, this fact may be related to the improved textural properties of the Al-PILCs when compared to the unpillared solids.

As might have been expected, the considerable platinum loading (2.3 wt.%) and catalyst preparation procedure (wet impregnation) used in this work resulted in relatively large platinum crystallites. Similar results were obtained by Parulekar and Hightower [29] by impregnating (0.5 wt.% Pt) an Al-pillared bentonite upon calcination at 773 K. In this case, it was reported that almost all the platinum was in the form of large crystallites in the 100–200 Å range on the external surface of the Al-PILC. On the other hand, Doblin et al. [28] observed by transmission electron microscopy (TEM) platinum particles with diameters of 20–50 Å on a low-loading (0.16 wt.%) Pt/Al-pillared montmorillonite catalyst prepared by ion exchange and calcined in flowing oxygen at 623 K.

3.2. Catalytic activity: influence of the ketone nature on the light-off curves

The light-off curves for acetone and MEK combustion over the Pt/SBhec-Al and Pt/CHmont-Al catalysts are shown in Fig. 2. In the same way, the results obtained in the combustion of the two ketones over the Pt/BAsap-Al and Pt/BAsap catalysts are plotted in Fig. 3. It can be seen that the temperatures required

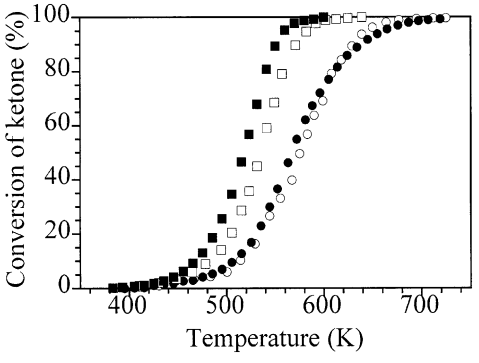

Fig. 2. Light-off curves for acetone combustion over Pt/SBhec-Al (○) and Pt/CHmont-Al (□) and MEK combustion over Pt/SBhec-Al (●) and Pt/CHmont-Al (■).

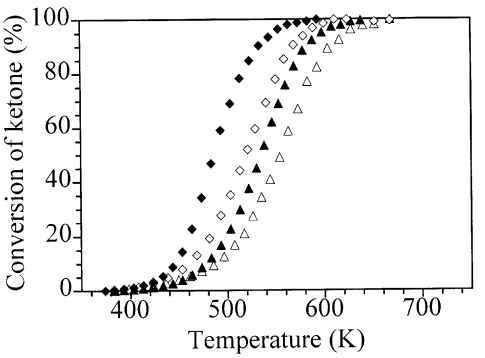

Fig. 3. Light-off curves for acetone combustion over Pt/BAsap-Al (△) and Pt/BAsap (◇) and MEK combustion over Pt/BAsap-Al (▲) and Pt/BAsap (◆).

for total combustion of acetone range between 625 K over Pt/BAsap and 725 K over Pt/SBhec-Al. In the case of MEK, these temperatures vary from 590 K over Pt/BAsap to 720 K over Pt/SBhec-Al. Little work has been done on the catalytic combustion of carbonyl VOCs, and ketones in particular. As far as platinum-based catalysts are concerned, Pina et al. [30] found complete combustion of 1850–2900 ppmv MEK in air at 473 K over a 0.19 wt.% Pt/γ-Al_2O_3 catalytic membrane. This temperature is clearly lower than the above-mentioned ones for the Pt/Al-PILCs; we must emphasize, however, the relatively low GHSV of 3500 h^{-1} used by Pina et al. [30] compared to about 34 000 h^{-1} in our case. As regards acetone combustion, Sharma et al. [31] reported a conversion value that did not exceed 80% at 673 K when processing 550–2350 ppmv acetone in air over a 0.1 wt.% Pt/fluorinated carbon catalyst at GHSV of 3000–15 000 h^{-1}. On the other hand, O'Malley and Hodnett [32] found complete combustion of 1000 ppmv acetone in helium with 12 vol.% oxygen at 493 K over 0.5 wt.% Pt/β-zeolite and at about 515 K over silica and alumina-supported platinum (2 wt.%) catalysts. Unfortunately, the authors did not report the value of the GHSV used. On the whole, the comparison of these results indicates that platinum catalysts on clay-based supports are promising catalysts able to yield ketone combustion efficiencies comparable to those described in previous applications for a considerable variety of platinum catalysts.

It is clear from the results in Figs. 2 and 3 that MEK is easier to oxidize than acetone over the Pt/Al-PILCs

catalysts. Indeed, taking the temperature at which a ketone conversion of 50% (T_{50}) is achieved as the light-off temperature [30], it can be seen that the temperatures required for light-off range from 485 to 565 K and from 518 to 575 K for MEK and acetone combustion, respectively. The largest difference (33 K) between the T_{50} values for acetone and MEK combustion is obtained over the Pt/BAsap catalyst, which is also the most active, whereas this difference is only 10 K in the case of Pt/SBhec-Al, the least active of the four catalysts in this work.

It is generally considered that C–H bond activation is a crucial first step in the catalytic combustion of hydrocarbons [32–35]. The C–H bond broke first in every hydrocarbon is the weakest one, which is usually associated with the C–H bond having the lowest dissociation enthalpy [32,34]. Once the first bond is broken, sequential reactions leading to the formation of the combustion products are relatively easy [35]. Reasonable correlations have been found showing that, for a great variety of hydrocarbons, the lower the C–H bond dissociation enthalpy, the easier the combustion of the corresponding organic compound. These results have been considered to provide evidence that the strength of the weakest C–H bond in the hydrocarbon is an important factor determining reactivity [32–34]. The results obtained by O'Malley and Hodnett [32] are of special importance to this work. These authors found that the temperatures required for total acetone combustion over supported platinum catalysts are about 100 K lower than those required for total combustion of deuterated acetone. According to O'Malley and Hodnett [32], this behaviour is consistent with a slow step in the combustion mechanism in which a C–H bond is almost fully cleaved. Nevertheless, it should be noted that, as Burch et al. [35] recently pointed out, kinetic isotope experiments may not be able to distinguish between the breaking of C–H and O–H bonds, either of which will exhibit kinetic isotope effects. As concerns the two ketones considered in this work, the dissociation enthalpies of the weakest C–H bonds are 411.3 kJ mol^{-1} for acetone (H–CH_2COCH_3) and 386.2 kJ mol^{-1} for MEK (H–$CH(CH_3)COCH_3$) [36]. Consequently, a relationship may be established between the higher reactivity of MEK compared to acetone found in this work and the strength of the weakest C–H bond in these ketones.

3.3. Effect of pillaring and of the parent clay nature on the catalytic activity

On the basis of the T_{50} values corresponding to the light-off curves shown in Figs. 2 and 3, the following order of decreasing catalytic performance may be established regardless of the ketone nature: Pt/BAsap > Pt/CHmont-Al > Pt/BAsap-Al > Pt/SBhec-Al. The differences in the T_{50} values among catalysts may be as high as 80 K for MEK combustion and 60 K in the case of acetone combustion. These results reveal a marked effect of pillaring and of the parent clay nature on the catalytic activity. Indeed the platinum catalyst supported on the unpillared Ballarat saponite is clearly the most active one. When the support is an Al-PILC, the activity increases in the following order with the parent clay nature: hectorite, saponite, montmorillonite.

The evolution with time-on-stream of the acetone conversion at 573 K for the four platinum catalysts is presented in Fig. 4. On the whole, the catalysts exhibit a good maintenance of the catalytic activity. More specifically, the behaviour of the Pt/BAsap catalyst is worth mentioning since this sample combines high activity and an excellent stability, showing no decrease in the acetone conversion during the 24 h period of time-on-stream of the catalytic run. On the other hand, a small loss of activity with time-on-stream is apparent in the case of the Pt/SBhec-Al catalyst. As can be seen the conversion values in Fig. 4 are in good accordance with the ones that can be estimated from the respective light-off curves at 573 K in Figs. 2 and 3. This indicates

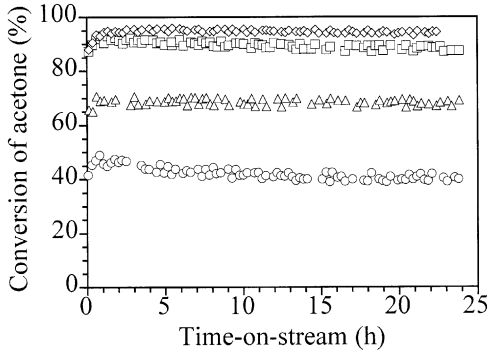

Fig. 4. Evolution of acetone conversion at 573 K with time-on-stream for Pt/SBhec-Al (○), Pt/CHmont-Al (□), Pt/BAsap-Al (△) and Pt/BAsap (◇).

that the above-mentioned order of catalysts activity is not influenced by stability differences among samples.

Given that all the catalytic runs were carried out using the same W_{Pt}/F_{in} ratio, it is obvious that the first issue which has to be considered in order to rationalize the behaviour of the several catalysts is platinum dispersion. It should be noted that estimation of the metallic dispersion from crystallite size measurements is unreliable due to the well-known limitations of the XRDLB technique [37]. Bearing this in mind, the results included in Table 1 indicate that there are no great differences between the mean platinum crystallite diameters exhibited by the Pt/Al-PILC catalysts. However, it is noteworthy that both Pt/BAsap and Pt/CHmont-Al catalysts show high activity and large platinum crystallite size. Papaefthimiou et al. [38], when studying the combustion of ethyl acetate over Pt/Al_2O_3 catalysts, found that the optimal platinum dispersion should be of the order 0.10–0.15, which corresponds to a platinum particle size of about 100 Å. It was also found that the turnover frequency (TOF) for ethyl acetate combustion increased significantly as the platinum particle size also increased in the 80–130 Å range.

In addition to the platinum dispersion, the state of the metallic surface is another important factor conditioning catalytic activity. This is a very complex subject which has been reported to depend on further factors such as the pre-treatment and reaction conditions [35,39–41], particle size effects [40,42,43] and effects of the preparation procedure and the presence of chloride on the initial dispersion, sintering and poisoning of platinum [44–49]. The main features of the hydrocarbon combustion reactions over platinum catalysts are accounted for by a dual-site model, where catalytic activity depends on the distribution of the metal between a dispersed and a crystalline phase [39,40,43,45]. The dispersed phase contains less active oxidized platinum in the form of PtO, PtO_2, [Pt^{IV}]-support surface complexes or chloride containing complexes such as [$Pt^{IV}(OH)_xCl_y$] and [$Pt^{IV}O_xCl_y$], depending on the case. On the other hand, the crystalline phase interacts only weakly with the support and consists of highly active metallic platinum. The relative amount of the two phases depends on the support composition, the nature of the platinum precursor, the metal loading and the conditions of calcination and reduction of the catalyst [39,43]. From this point of view, the differences in catalytic activity found in this work among the several platinum catalysts might be primarily related to the differences in support composition, namely the nature of the parent smectite and the character, pillared or not, of the clay support. In this respect, the results recently reported by Hwang and Yeh [41] on Pt/silica–alumina catalysts are specially interesting in view of the fact that the pillars of the Al-PILCs may be considered as a hydroxy-aluminic phase keeping apart the clay silicate layers. Hwang and Yeh found platinum-oxide species on silica–alumina of up to six different chemical environments. They were assigned to PtO and PtO_2 dispersed on silica-rich grains, on alumina-rich grains and in cages at grain boundaries. It was found that as the Al_2O_3/SiO_2 ratios of the silica–alumina supports increased the species on alumina-rich grains and in cages were favoured. These species were significantly more difficult to reduce that the ones dispersed on silica-rich grains, as evidenced by temperature-programmed reduction (TPR) experiments [41]. On the basis of these findings, the pillars of the Al-PILC supports may be considered as alumina-rich areas as well, which would favour the formation of a dispersed and less active oxidized platinum phase. It should be noted that, as mentioned earlier, the micropore volume loss that takes place on preparing the Pt/Al-PILCs catalysts suggests that some metallic precursor species may have reached the inner porous network of the support. In contrast, it is likely that on using an unpillared clay support the contribution of the crystalline metallic platinum phase be higher than in the case of the Al-PILCs. Accordingly, the higher catalytic activity exhibited by the Pt/BAsap catalyst compared to the Pt/Al-PILC ones might be due at least in part to a larger contribution of the crystalline platinum phase in favour of Pt/BAsap.

Another important issue is the possible influence of the acid properties of the support on the catalytic activity. Pt/Al-PILCs catalysts have previously received considerable attention in view of their potential use in *n*-alkane hydroconversion processes [28,29,50–53]. As in our case, remarkable differences in catalytic performance among samples have been found in these applications depending on the nature of the starting clay. Indeed, it has been reported that clays with tetrahedral Al for Si isomorphous substitutions (beidellites, saponites) give rise to more active

and selective *n*-alkane hydroisomerization catalysts than clays with octahedral isomorphous substitutions (hectorites, montmorillonites) [50,51]. It should be noted that in this type of reactions the PILC-support promotes the proton-catalysed steps of the overall process. Hence, the catalytic activity order of the various smectites has been accounted for by the presence of strong Si–OH $\cdots$ Al acid sites in Al-pillared beidellites and saponites as a result of the proton attack of tetrahedral Si–O–Al bonds. These strong Brönsted acid sites are almost non-existent in clays without significant tetrahedral Al for Si substitutions (hectorite and montmorillonite) [5,51–53]. From this point of view, it seems that in our case there is a trend opposite to the existing one in hydroconversion reactions because except for Pt/SBhec-Al, the catalytic activity for the ketone combustion increases in the following order with support nature: Al-pillared saponite < Al-pillared montmorillonite < unpillared saponite. It is well known that unpillared smectite clays usually show only very weak Brönsted acidity [5]; accordingly, it can be suggested that the Brönsted acid properties of the support might have a negative effect on the performance of Pt/Al-PILCs catalysts for ketone combustion reactions.

As far as hydrocarbon combustion reactions over platinum-based catalysts are concerned, it has been proposed that the complete elimination of the Lewis acid sites of Pt/Al_2O_3 catalysts could diminish their susceptibility to coking during the combustion of alkenes [54]. On the other hand, positive effects of the acidic properties of the supports have been claimed for the combustion of alkanes as propane [55] and *n*-pentane [56] over supported platinum catalysts. In our case, the carbonyl character of the VOCs involved may be a very important factor since both acetone and MEK can undergo base- or acid-catalysed aldol condensation reactions with the production of strongly bound surface species [34]. Indeed, Flego and Perego [57] have proposed a mechanism for acetone aldol condensation over acidic solids by which, initially, a molecule of acetone reacts with another protonated acetone molecule interacting with a Brönsted acid site. In the presence of very acidic catalysts and high temperatures, consecutive dehydratation, acetone addition and cyclization reactions can lead to the formation of relatively complex aromatic compounds which are coke precursors [57]. Under these circumstances, it may be expected that over the more acid catalysts (Pt/BAsap-Al) the aldol condensation reactions of the ketones compete to some extent with their complete oxidation, thus contributing to a comparatively lower combustion activity.

4. Conclusions

In this work, Al-pillared smectite clays were considered as supports of platinum catalysts for the catalytic combustion of two carbonyl VOCs, acetone and MEK. A hectorite, a montmorillonite and a saponite were subjected to intercalation with aluminium oligomers to synthesize the Al-PILC supports upon calcination. These solids as well as the unpillared saponite were wet-impregnated with an aqueous solution of $[Pt(NH_3)_4]Cl_2$, dried and calcined in air at 773 K in order to prepare the platinum catalysts (2.3 wt.% Pt). Characterization by means of nitrogen adsorption at 77 K revealed that the presence of platinum modified the textural properties of the supports. Whereas the mesopore volumes remained almost unchanged, the pore volume loss that the catalysts suffered affected almost exclusively the micropores of the Al-PILCs, indicating that some platinum species have reached the inner porous network of the supports. After reduction in hydrogen at 773 K the presence of poorly dispersed metallic platinum with mean crystallite diameters in the 70–100 Å range was detected by XRD.

On the basis of the light-off curves for the ketones combustion over the platinum catalysts previously reduced in hydrogen at 773 K, the temperatures required for total combustion ranged from 625 to 725 K for acetone and from 590 to 720 K for MEK. Taking into account the relatively high GHSV used in this work, these results imply ketone combustion efficiencies comparable to those previously reported for a considerable variety of platinum catalysts on conventional supports. Moreover, the Pt/Al-PILCs catalysts exhibited a good stability as evidenced by a series of long catalytic runs performed at constant combustion temperature. Whatever the catalyst considered, it has been found that MEK is more easy to oxidize than acetone. This behaviour has been related to the lower strength of the weakest C–H bond in MEK compared to acetone.

Remarkable differences in catalytic performance among the platinum catalysts were found depending on the pillared or unpillared character of the support and the starting smectite clay used. As a result, regardless of the ketone nature, the following order of decreasing catalytic activity was established with respect to the support nature: unpillared saponite > Al-pillared montmorillonite > Al-pillared saponite > Al-pillared hectorite. This result has been discussed in terms of the possible effect of the support composition on the distribution of platinum between a dispersed and a crystalline phase. Moreover, the possibility of the Brönsted acid properties of the support having a negative effect on the activity of the catalysts for ketone combustion reactions can be suggested.

Acknowledgements

Financial support by MEC (CICYT-QUI97-1040-CO3-02) and Departamento de Educación y Cultura del Gobierno de Navarra (Orden Foral 143/1998) are gratefully acknowledged. MAV carried out a part of this work during a postdoctoral stay at the Pierre and Marie Curie University, financed by the European Commission (TMR Marie Curie Training Grants ref. ERB4001GT964051 and ERB4001GT974744).

References

[1] T.J. Pinnavaia, Science 220 (1983) 365.
[2] F. Figueras, Catal. Rev. 30 (1988) 457.
[3] D.E.W. Vaughan, Catal. Today 2 (1988) 187.
[4] K. Othsuka, Chem. Mater. 9 (1997) 2039.
[5] J.-F. Lambert, G. Poncelet, Topics Catal. 4 (1997) 43.
[6] P. Cool, E.F. Vansant, in: H.G. Karge, J. Weitkamp (Eds.), Molecular Sieves — Science and Technology, Vol. 1, Synthesis, Springer, Berlin, 1998, p. 265.
[7] A. Vaccari, Catal. Today 41 (1998) 53.
[8] A. Gil, L.M. Gandía, M.A. Vicente, Catal. Rev. 42 (2000) 145.
[9] G.W. Brindley, in: G.W. Brindley, G. Brown (Eds.), Crystal Structures of Clay Minerals and their X-ray Identification, Mineralogical Society, Colchester, 1984, p. 169.
[10] S. Cheng, Catal. Today 49 (1999) 303.
[11] A. Gil, M. Montes, Langmuir 10 (1994) 291.
[12] N.D. Hutson, M.J. Hoekstra, R.T. Yang, Micropor. Mesopor. Mater. 28 (1999) 447.
[13] A. Gil, M.A. Vicente, L.M. Gandía, Micropor. Mesopor. Mater. 34 (2000) 115.
[14] M.L. Occelli, J.A. Bertrand, S.A.C. Gould, J.M. Dominguez, Micropor. Mesopor. Mater. 34 (2000) 195.
[15] M.A. Vicente, J.-F. Lambert, Phys. Chem. Chem. Phys. 1 (1999) 1633.
[16] L.M. Gandía, M.A. Vicente, A. Gil, Appl. Catal. A 196 (2000) 281.
[17] M.S. Jennings, N.E. Krohn, R.S. Berry, M.A. Palazzolo, R.M. Parks, K.K. Fidler, Catalytic Incineration for Control of VOC Emissions, Noyes Publications, Park Ridge, NJ, 1985.
[18] N. Mukhopadhyay, E.C. Moretti, Current and Potential Future Industrial Practices for Reducing and Controlling Volatile Organic Compounds, Center for Waste Reduction Technologies, American Institute of Chemical Engineers, New York, 1993.
[19] J.J. Spivey, Catalysis, Vol. 8, The Royal Society of Chemistry, Cambridge, 1989, p.157.
[20] R. Prasad, L.A. Kennedy, E. Ruckenstein, Catal. Rev. 26 (1984) 1.
[21] M.F.M. Zwinkels, S.G. Järås, P.G. Menon, T.A. Griffin, Catal. Rev. 35 (1993) 319.
[22] L. Storaro, R. Ganzerla, M. Lenarda, R. Zanoni, J. Mol. Catal. A 97 (1995) 139.
[23] A. Gil, M.A. Vicente, R. Toranzo, M.A. Bañares, L.M. Gandía, J. Chem. Technol. Biotechnol. 72 (1998) 131.
[24] A. Gil, P. Grange, Langmuir 13 (1997) 4483.
[25] G. Horvath, K. Kawazoe, J. Chem. Eng. Jpn. 16 (1983) 470.
[26] H.P. Klug, L.E. Alexander, X-Ray Diffraction Procedures, Wiley, New York, 1974, p. 618.
[27] S.J. Gregg, K.S.W. Sing, Adsorption, Surface Area and Porosity, Academic Press, London, 1991.
[28] C. Doblin, J.F. Mathews, T.W. Turney, Appl. Catal. 70 (1991) 197.
[29] V.N. Parulekar, J.W. Hightower, Appl. Catal. 35 (1987) 263.
[30] M.P. Pina, S. Irusta, M. Menéndez, J. Santamaría, R. Hughes, N. Boag, Ind. Eng. Chem. Res. 36 (1997) 4557.
[31] R.K. Sharma, B. Zhou, S. Tong, K.T. Chuang, Ind. Eng. Chem. Res. 34 (1995) 4310.
[32] A. O'Malley, B.K. Hodnett, Catal. Today 54 (1999) 31.
[33] V.D. Sokolovskii, Catal. Rev. 32 (1990) 1.
[34] G. Busca, E. Finocchio, G. Ramis, G. Ricchiardi, Catal. Today 32 (1996) 133.
[35] R. Burch, D.J. Crittle, M.J. Hayes, Catal. Today 47 (1999) 229.
[36] D.R. Lide (Ed.), CRC Handbook of Chemistry and Physics, 75th Edition, CRC Press, Boca Raton, 1994.
[37] J.T. Richardson, Principles of Catalyst Development, Plenum Press, New York, 1989, p. 162.
[38] P. Papaefthimiou, T. Ioannides, X.E. Verykios, Appl. Catal. B 13 (1997) 175.
[39] J. Völter, G. Lietz, H. Spindler, H. Lieske, J. Catal. 104 (1987) 375.
[40] R. Burch, P.K. Loader, Appl. Catal. B 5 (1994) 149.
[41] C.-P. Hwang, C.-T. Yeh, J. Catal. 182 (1999) 48.
[42] P. Briot, A. Auroux, D. Jones, M. Primet, Appl. Catal. 59 (1990) 141.
[43] R.F. Hicks, H. Qi, M.L. Young, R.G. Lee, J. Catal. 122 (1990) 280.
[44] J. Barbier, D. Bahloul, P. Marécot, Catal. Lett. 8 (1991) 327.
[45] P. Marécot, A. Fakche, B. Kellali, G. Mabilon, M. Prigent, J. Barbier, Appl. Catal. B 3 (1994) 283.

[46] P. Reyes, M. Oportus, G. Pecchi, R. Fréty, B. Moraweck, Catal. Lett. 37 (1996) 193.
[47] S. Feast, M. Englisch, A. Jentys, J.A. Lercher, Appl. Catal. A 174 (1998) 155.
[48] Z.C. Zhang, B.C. Beard, Appl. Catal. A 188 (1999) 229.
[49] A. Borgna, T.F. Garetto, C.R. Apesteguía, F. Le Normand, B. Moraweck, J. Catal. 186 (1999) 433.
[50] R. Molina, S. Moreno, A. Vieira-Coelho, J.A. Martens, P.A. Jacobs, G. Poncelet, J. Catal. 148 (1994) 304.
[51] S. Moreno, R. Sun Kou, G. Poncelet, J. Catal. 162 (1996) 198.
[52] S. Moreno, R. Sun Kou, G. Poncelet, J. Phys. Chem. B 101 (1997) 1569.
[53] S. Moreno, R. Sun Kou, R. Molina, G. Poncelet, J. Catal. 182 (1999) 174.
[54] V. Labalme, B. Béguin, F. Gaillard, M. Primet, Appl. Catal. A 192 (2000) 307.
[55] A. Ishikawa, S. Komai, A. Satsuma, T. Hattori, Y. Murakami, Appl. Catal. A 110 (1994) 61.
[56] W. Hua, Z. Gao, Appl. Catal. B 17 (1998) 37.
[57] C. Flego, C. Perego, Appl. Catal. A 192 (2000) 317.